Floquet Symmetry-Protected Topological Phases in Cold-Atom Systems

I.-D. Potirniche, A. C. Potter, M. Schleier-Smith, A. Vishwanath, and N. Y. Yao

Phys. Rev. Lett. **119**, 123601 — Published 21 September 2017

DOI: 10.1103/PhysRevLett.119.123601

Floquet symmetry-protected topological phases in cold atomic systems

I.-D. Potirniche,[1] A. C. Potter,[2] M. Schleier-Smith,[3] A. Vishwanath,[1,4] and N. Y. Yao[1]

[1]*Department of Physics, University of California, Berkeley, California, 94720, USA*
[2]*Department of Physics, The University of Texas at Austin, Austin, Texas 78712, USA*
[3]*Department of Physics, Stanford University, Stanford, California 94305, USA*
[4]*Department of Physics, Harvard University, Cambridge, MA 02138, USA*

(Dated: July 19, 2017)

We propose and analyze two distinct routes toward realizing interacting symmetry-protected topological (SPT) phases via periodic driving. First, we demonstrate that a driven transverse-field Ising model can be used to engineer complex interactions which enable the emulation of an equilibrium SPT. This phase remains stable only within a parametric time scale controlled by the driving frequency, beyond which its topological features break down. To overcome this issue, we consider an alternate route based upon realizing an intrinsically Floquet SPT phase that does not have any equilibrium analogue. In both cases, we show that disorder, leading to many-body localization, prevents runaway heating and enables the observation of coherent quantum dynamics at high energy densities. Furthermore, we clarify the distinction between the equilibrium and Floquet SPT phases by identifying a unique micro-motion-based entanglement spectrum signature of the latter. Finally, we propose a unifying implementation in a one dimensional chain of Rydberg-dressed atoms and show that protected edge modes are observable on realistic experimental time-scales.

The discovery of topological insulators—materials which are insulating in their interior but can conduct on their surface—has led to a multitude of advances at the interface of condensed matter physics and materials engineering [1–5]. At their core, such insulators are characterized by the existence of non-trivial topology in their underlying single-particle electronic band structure [6, 7]. Generalizing our understanding of topological phases to the presence of strong many-body interactions represents one of the central questions in modern physics. Some of the simplest generalizations that have emerged along this direction are symmetry protected topological (SPT) phases [8–10], which represent the minimal extension of topological band insulators to include many-body correlations. Featuring short-range entanglement, SPT phases do not exhibit anyonic excitations in their bulk, but nevertheless possess protected edge modes on their surface; as a result, they represent a particularly fertile ground for studying the interplay between symmetry, topology, and interactions.

While indirect signatures of certain ground state SPT's have been observed in the solid state [11–13], directly probing the quantum coherence of their underlying edge modes represents an outstanding experimental challenge. In principle, cold atomic quantum simulations could offer a powerful additional tool set—including locally-resolved measurements and interferometric protocols—for probing the robustness of edge modes and systematically exploring their stability to specific perturbations [14–18]. Moreover, such platforms could also enable the controlled storage and transmission of quantum information [19–21]. Despite these advantages, and owing to the complexity of typical model SPT Hamiltonians, it remains difficult to engineer and stabilize SPT phases in cold atomic systems.

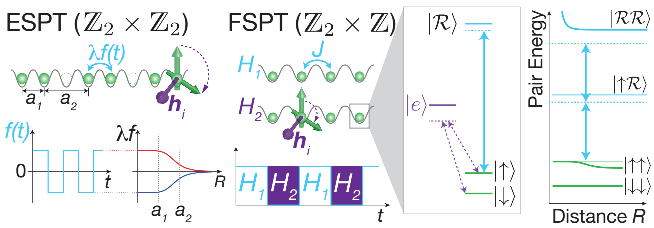

FIG. 1. A 1D array of atoms is trapped in an optical lattice or tweezer array. Ising interactions for pseudo-spin states $|\downarrow\rangle, |\uparrow\rangle$ are generated by optically coupling $|\uparrow\rangle$ to Rydberg state $|\mathcal{R}\rangle$ (solid blue arrows). Random fields h_i are generated by a spatially varying Raman coupling (dotted purple arrows) between $|\downarrow\rangle$ and $|\uparrow\rangle$. While emulating the ESPT phase requires a dimerized chain with Ising couplings $\lambda f(t)$ of dynamically switchable sign, the FSPT phase is simulated simply by alternating between two Hamiltonians consisting of Ising interactions (H_1) and a disordered transverse field (H_2).

One approach to this challenge is to emulate the complex interactions giving rise to static, equilibrium SPT (ESPT) phases by periodically driving a simpler Hamiltonian at frequencies much larger than its intrinsic energy scales [22]. In addition to this approach, seminal results on classifying driven (Floquet) phases [23–28] have also shown that there exist Floquet-SPT's (FSPT) which are inherently dynamical and have no static analogue. Interestingly, such an FSPT can be realized at driving frequencies that are *comparable* to the energy scales of the bare Hamiltonian.

The power of periodic driving for engineering topological phases has been extensively explored in cold-atom [29–31], solid-state [32–34], and photonic [35, 36] systems. For cold atoms, where Floquet control has so far been applied only to single-particle band structures [29–31, 37–39], recent advances in optically controlling interactions [40–47] offer new opportunities for accessing strongly correlated phases [48–51]. Notably, coherent spin-spin interactions with a range of several microns [42, 43, 46, 47] can be introduced via Rydberg dressing [42–44, 46, 47, 52–55]. However, prospects for modulating such dressing light in order to Floquet engineer many-body Hamiltonians has remained largely unexplored.

This owes, in part, to the difficulty of generating quantum coherent order in an interacting Floquet system which will typically absorb energy from the driving field, eventually heating to a featureless infinite temperature state [56, 57]. This difficulty is further exacerbated for isolated atomic systems, where the lack of coupling to an external bath renders the system incapable of releasing excess energy and entropy [58]. A fruitful strategy for combating such heating is to harness many-body localization (MBL) [23, 59–62], which has been predicted to stabilize quantum coherent behavior without the need for stringent cooling or adiabatic preparation of low temperature many-body states [19–21, 63].

In this Letter, we propose to exploit periodically driven interactions to realize two distinct non-equilibrium MBL SPT phases in a one-dimensional array of cold atoms (Fig. 1). Driving the interaction term of a transverse-field Ising model (TFIM) enables the emulation of an ESPT whose edge modes are protected by an emergent $\mathbb{Z}_2\times\mathbb{Z}_2$ symmetry [22]. This phase remains stable only within a parametric time scale controlled by the driving frequency, beyond which its topological features break down. Alternatively, toggling between Hamiltonians with solely Ising interactions or purely transverse fields yields an intrinsically dynamical FSPT which has no equilibrium analogue. We explore the stability of both phases to long-range interactions and provide a detailed experimental blueprint using Rydberg-dressed atoms.

ESPT Phase—Inspired by pioneering work on emulating static phases in driven systems [22, 32, 33, 64–68], we first consider the realization of a many-body localized version of the Haldane phase [69]. This SPT phase can be protected by a discrete dihedral symmetry, $\mathbb{Z}_2\times\mathbb{Z}_2$, and exhibits boundary modes that are odd under the symmetry; these edge modes behave as decoupled spin-1/2 degrees of freedom that are robust to any perturbation which preserves the symmetry.

We begin by examining the robustness of the edge modes in a periodically driven and dimerized spin chain (Fig. 1):

$$H_0(t)=\sum_{i=1}^{N}h_i\sigma_i^x+\sum_{i=1}^{N-1}f(t)\lambda_i\sigma_i^z\sigma_{i+1}^z+V_x\sigma_i^x\sigma_{i+1}^x,\quad (1)$$

where N represents an even number of spins, σ_i^α are the Pauli operators on site i, $\lambda_{2k+1}=\lambda_1$, $\lambda_{2k}=\lambda_2$ (with $\lambda_1,\lambda_2>0$) and $f(t)=\omega\cos(\omega t)$ is the driving function

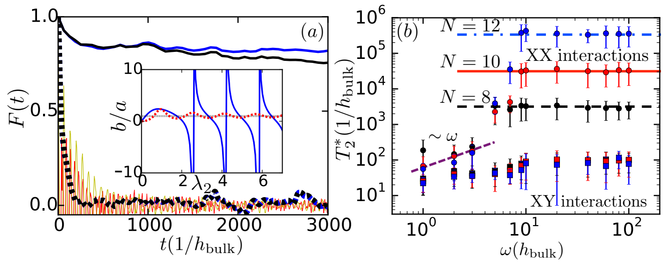

FIG. 2. ESPT phase—(a) $F^\alpha(t)$ for $N=10$ spins with $\omega=100$, $V_x=0.05$, $V_y=0$, $\lambda_1=1.54$ and $\lambda_2=0.69$, yielding $b(\lambda_1,\lambda_2)/a(\lambda_1,\lambda_2)\sim 10$. Almost overlapping dotted lines represent the clean undisordered case (black and blue for F^z and F^x, respectively). Solid lines correspond to strong on-site disorder, with thick black and blue lines for F^z and F^x in the dimerized case and thin solid yellow and red lines for F^z and F^x in the un-dimerized case. (inset) Ratio $b(1,\lambda_2)/a(1,\lambda_2)$ in the dimerized (solid blue) and the un-dimerized (dotted red) models. The SPT phase corresponds to $b/a>1$ (delimited by the dotted black line). (b) T_2^* as a function of frequency and system size [71]. As ω is increased for $V_x=0.05$ (circles), T_2^* saturates consistent with being bounded by $T_2^*\sim\min(\mathcal{O}(\omega),e^{\mathcal{O}(N)})$. Adding generic interactions, $V_y\sum_i\sigma_i^y\sigma_{i+1}^y$ with $V_y=0.2$ (squares), leads to a breakdown of the edge coherence for all parameters.

[70]. For $V_x=0$, the model is non-interacting and exhibits edge dynamics which never decohere [22]. Here, we first verify that the SPT phase remains stable under the addition of short-range interactions $V_x\neq 0$ that preserve the dihedral symmetry (generated by products of σ_i^x on the even and odd sites). We then assess the effects of more generic, longer range, interactions.

In the limit of large driving frequencies ω, the dynamics are described by an effective time-independent Floquet Hamiltonian, $H_{\rm F}$, which can be constructed perturbatively in orders of $1/\omega$ using a Magnus expansion [72–74]. At leading order, we obtain the time-averaged Floquet Hamiltonian [71]

$$\begin{aligned}H_{\rm F}^{(0)}&=\sum_{i=1}^{N}h_ia(\lambda_1,\lambda_2)\sigma_i^x-\sum_{i=2}^{N-1}h_ib(\lambda_1,\lambda_2)\sigma_{i-1}^z\sigma_i^x\sigma_{i+1}^z \quad (2)\\&+V_xJ_0(2\lambda_2)(\sigma_1^x\sigma_2^x+\sigma_{N-1}^x\sigma_N^x)\\&+V_x\sum_{i=2}^{N-2}\left[c(\lambda_{i+1})\sigma_i^x\sigma_{i+1}^x+d(\lambda_{i+1})\sigma_{i-1}^z\sigma_i^y\sigma_{i+1}^y\sigma_{i+2}^z\right],\end{aligned}$$

where $J_0(x)$ is the Bessel function of the first kind, $a(\lambda_1,\lambda_2)=\frac{1}{2}\left[J_0\left(2(\lambda_1-\lambda_2)\right)+J_0(2(\lambda_1+\lambda_2))\right]$, $b(\lambda_1,\lambda_2)=J_0(2(\lambda_1-\lambda_2))-a(\lambda_1,\lambda_2)$, $c(\lambda)=\frac{1}{2}\left[1+J_0(4\lambda)\right]$, and $d(\lambda)=1-c(\lambda)$. We have absorbed a factor of $\frac{J_0(2\lambda_1)}{a(\lambda_1,\lambda_2)}$ in the definitions of h_1 and h_N [75].

A few remarks are in order. First, the periodic driving, $f(t)$, effectively generates multi-spin interactions [Eqn. (2)] [22]. Secondly, while $H_{\rm F}^{(0)}$ exhibits a $\mathbb{Z}_2\times\mathbb{Z}_2$

symmetry, the parent Hamiltonian [Eqn. (1)] possesses only a smaller $\mathbb{Z}_2$ symmetry group, indicating that the "emergent" dihedral symmetry of $H_{\mathrm{F}}^{(0)}$ must be broken at higher orders in the Magnus expansion [71]. Finally, the $V_x = 0$ limit of Eqn. (2) describes a pair of decoupled 1D p-wave superconductors [76] and harbors two simple limits: for $a(\lambda_1, \lambda_2) > b(\lambda_1, \lambda_2)$, the ground state is a trivial insulator, while for $a(\lambda_1, \lambda_2) < b(\lambda_1, \lambda_2)$, the ground state is a bosonic SPT insulator. The key signature of this latter ESPT phase is the existence of protected modes localized around the boundary of the system. Crucially, the λ_1, λ_2-dimerization of the Ising interaction enables us to arbitrarily tune the correlation length of the edge mode (inset of Fig. 2a), leading to coherent dynamics with significantly higher fidelity than those of the un-dimerized TFIM [22].

To characterize the edge coherence, we introduce the trace fidelity $F^\alpha(t) = \frac{1}{Z}\mathrm{Tr}\left[e^{-\beta H(t)}\Sigma^\alpha(t)\Sigma^\alpha(0)\right]$ as a function of time, where Z is the partition function, $\beta = 1/k_{\mathrm{B}}T$, and Σ^α are the zero correlation length edge operators $\Sigma^x = \sigma_1^x\sigma_2^z$, $\Sigma^y = \sigma_1^y\sigma_2^z$, and $\Sigma^z = \sigma_1^z$. This autocorrelation function at infinite temperature will serve as a proxy for the coherence time. Furthermore, since we are interested in coherent MBL-protected dynamics at finite energy densities, from hereon we add strong disorder to the system via random on-site fields h_i [77].

As alluded to above, there are two mechanisms of edge spin decoherence introduced by interactions: 1) scattering with thermal excitations and 2) breaking of the $\mathbb{Z}_2 \times \mathbb{Z}_2$ symmetry. While the first is ameliorated via MBL (Fig. 2a), the second is intrinsic to the stroboscopic approach—the ESPT is stable only up to a finite parametric time scale, $T_{2,\mathrm{symm}}^* \sim (h^2/\omega)^{-1}$, beyond which the protecting symmetry is broken.

The first effect is reminiscent of similar discussions in the static context [19–21], where disorder can localize thermal bulk excitations and suppress scattering. Since the edge operators are odd under the $\mathbb{Z}_2 \times \mathbb{Z}_2$ symmetry, their dressed MBL-counterparts will not appear in the effective "l-bit" Hamiltonian [60, 61] and dephasing occurs solely via coupling to the other edge mode [21] on a time scale that is exponential in system size, $T_{2,\mathrm{MBL}}^* \sim e^{\mathcal{O}(N)}$[78], as depicted in Fig. 2b. Thus, so long as the effective dynamics are described by $H_{\mathrm{F}}^{(0)}$, one finds that even in the interacting, periodically driven system, disorder can lead to a revival of the coherence time (Fig. 2a).

This MBL enhancement of edge coherence is cut off by the fact that the first order Magnus correction, $H_{\mathrm{F}}^{(1)}$, breaks the $\mathbb{Z}_2 \times \mathbb{Z}_2$ symmetry. For time scales $t > T_{2,\mathrm{symm}}^*$, even though bulk excitations remain many-body localized, there is no symmetry protecting the edge operators, which can then scatter locally. Thus, for a finite size system, decoherence in the presence of interactions that preserve the dihedral symmetry occurs on a time scale $T_2^* \sim \min(T_{2,\mathrm{MBL}}^*, T_{2,\mathrm{symm}}^*) \sim \min(e^{\mathcal{O}(N)}, \mathcal{O}(\omega/h^2))$ as illustrated in Fig. 2b.

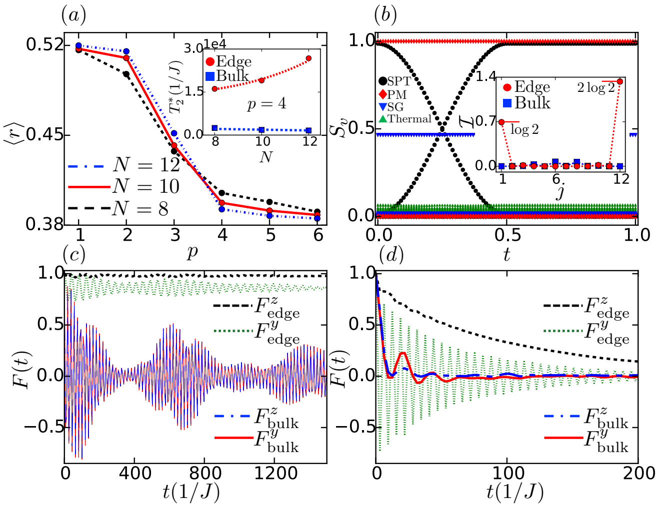

FIG. 3. FSPT phase—(a) The $\langle r\rangle$ ratio as a function of the power law exponent p for a chain with periodic boundary conditions. The h_i's are sampled from the uniform distribution $[0.1, 0.9]$ and $T = \pi$ (in units of $J = 1$). There is an MBL-delocalization phase transition around $p_c \approx 3.5$. (inset) T_2^* as a function of N, where the edge coherence is fit to $\sim N^4$. (b) The entanglement spectrum micro-motion for $N = 12$. The parameters (p, T, J, W) are: $(4, \pi, 1, 1)$ for the SPT; $(1, \pi, 1, 1)$ for the thermal behavior; $(4, \pi, 0.05, 0.8)$ for the paramagnet; $p = 4$, $T = \pi$, $J = 0.5$, $h \in [0.5, 1]$ for the spin glass. (inset) Mutual information $\mathcal{I}(i, j) = S_i + S_j - S_{ij}$ (where S is the von Neumann entropy) within the SPT phase: $\mathcal{I}(1, j)$ (red circles) and $\mathcal{I}(6, j)$ (blue squares) [71]. (c) $F^y(t)$ and $F^z(t)$ for the edge and the bulk in a system of $N = 10$ spins for the model in Eqn. 3. The bulk curves are almost overlapping. (d) Same as in (c), but with an additional term, $V_x \sum_i \sigma_i^x \sigma_{i+1}^x$ $(V_x = 0.3)$ added to H_1.

The addition of a more generic symmetry-breaking interaction term, such as $V_y \sum_i \sigma_i^y \sigma_{i+1}^y$ or a long-range power-law tail, breaks the $\mathbb{Z}_2 \times \mathbb{Z}_2$ symmetry at lowest order in the Magnus expansion. In this case, there is no parametric time scale where we expect ESPT dynamics (i.e. $T_{2,\mathrm{symm}}^* \sim \mathcal{O}(1)$), and the edge modes rapidly decohere via local scattering (Fig. 2b).

FSPT Phase—To obtain edge modes with coherence that persists to arbitrary times and is robust to long-range interactions, we now turn to the realization of an intrinsically Floquet SPT phase. We engineer an FSPT protected by both $\mathbb{Z}_2$ symmetry and periodic driving which cannot exist in equilibrium [24–28]. Consider the stroboscopic Hamiltonian

$$H(t) = \begin{cases} H_1 = \displaystyle\sum_{i \neq j} \frac{J}{|R_i - R_j|^p} \sigma_i^z \sigma_j^z & \text{if} \quad 0 \le t < T/2 \\ H_2 = \displaystyle\sum_{i=1}^{N} h_i \sigma_i^x & \text{if} \quad T/2 \le t < T, \end{cases} \tag{3}$$

where $R_i = i$ is the position of the i^{th} spin and $h_i \in [0, W]$. The protecting symmetries are the product of σ_x on all sites ($\mathbb{Z}_2$) and discrete translations in time ($\mathbb{Z}$). The unitary evolution under $H(t)$ is given by $U(t) = \mathcal{T}\exp\left(-i\int_0^T H(t)dt\right)$ and the Floquet operator by $U = U(T)$. Building upon previous studies [23, 65, 79, 80], we expect to observe the FSPT phase at $\frac{JT}{2} \approx \frac{\pi}{2}$ [71].

Since the disorder strength is limited to $W \lesssim 1/T$ by the periodic structure of the binary drive [71], the system cannot be localized for arbitrarily strong interactions. By computing the level-statistics ratio $\langle r\rangle$ [81] as a function of the power-law exponent p (Fig. 3a), we observe a clear MBL-delocalization phase transition at $p_c \approx 3.5$ [82]. For the remainder of the text, we set $p = 4$ as a computationally tractable model within the MBL phase.

To probe the nature of edge coherence in the FSPT phase, we again compute the trace fidelity $F^\alpha = \frac{1}{2^N}\mathrm{Tr}\left[\sigma_i^\alpha(t)\sigma_i^\alpha(0)\right]$. As depicted in the inset of Fig. 3a, and similar to the ESPT phase, the edge spin exhibits a significantly longer coherence time than bulk spins. However, a crucial difference emerges in the scaling with N. For long-range interactions, the coherence time of the ESPT phase scales independently of the system size, $T_2^* \sim \mathcal{O}(1)$, whereas the FSPT exhibits a quartic scaling $T_2^* \sim \mathcal{O}(N^4)$ (owing to the $1/R^4$ power-law interactions between the two edge modes), as shown in the inset of Fig. 3a).

To further distinguish between the topological features of the ESPT and FPST phases, we introduce a novel micro-motion-based entanglement spectrum signature of the latter [26]. In particular, for an eigenstate $|\psi\rangle$ of the Floquet operator U, we compute the entanglement spectrum, $\{\eta_i(t)\}$, associated with the half-chain cut of $|\psi(t)\rangle = U(t)\,|\psi\rangle$ for $0 \le t \le T$. By Schmidt decomposing $|\psi(t)\rangle = \sum_{i=1}^{2^{N/2}} \eta_i(t)\,|\mathrm{Left}_i(t)\rangle\otimes|\mathrm{Right}_i(t)\rangle$, we obtain $\{\eta_i(t)\}$ across the two sets, $\{|\mathrm{Left}_i(t)\rangle\}$ and $\{|\mathrm{Right}_i(t)\rangle\}$, which span the Hilbert spaces of the left and right halves of the chain. Unlike in equilibrium, where a single snapshot of the entanglement spectrum shows the existence of topological edge modes, we find that, at any given time t, the spectrum is trivial and there is no signature of FSPT order (Fig. 3b). However, by following the micro-motion evolution of the spectrum over a single Floquet period, we can robustly identify the topological signature of the FSPT phase [26].

To see this, we note that the entanglement spectrum is gapped at $t = 0$ and $t = T$ which allows us to associate an SPT invariant to each non-trivial band—namely, the $\mathbb{Z}_2$ symmetry charge of the corresponding Schmidt states, $\langle\mathrm{Left}_i(t)|\prod_j \sigma_j^x\,|\mathrm{Left}_i(t)\rangle = \pm 1$. There exists a band crossing during the micro-motion (Fig. 3b), pointing to the fact that the charges of each band are flipping during a Floquet period. This difference between the initial and final $\mathbb{Z}_2$ charges cannot be altered without closing the entanglement gap, suggesting that the band-crossing is, in fact, a robust feature of FSPT order. Indeed, this non-trivial behavior is absent in the paramagnetic and spin glass phases (Fig. 3b).

Experimental realization—Both the ESPT and FPST Hamiltonians can be implemented in a chain of Rydberg-dressed alkali atoms [43, 44, 46, 49, 50] trapped in a 1D optical lattice or tweezer array [83, 84] (Fig. 1). The spin degree of freedom is formed by two ground hyperfine states, with a resonant Raman coupling of spatially varying Rabi frequency h_i simulating the on-site transverse fields. Random fields can be formed by optical speckle disorder or with a spatial light modulator.

Strong spin-spin interactions are introduced by coupling state $|\uparrow\rangle$ to a Rydberg state $|\mathcal{R}\rangle$ with an off-resonant laser field of Rabi frequency Ω and detuning $\Delta > \Omega$. The result is an effective (dressed) Ising interaction [43, 55]

$$H_I = -\frac{\Omega^4}{8\Delta^3}\frac{1}{1+|R_i - R_j|^6/R_c^6}\sigma_i^z\sigma_j^z, \qquad (4)$$

where the interaction range $R_c = (-C_6/\Delta)^{1/6}$ depends on the van der Waals coefficient C_6 of the Rydberg-Rydberg interaction and is typically on the few-micron scale. At fixed lattice spacing a_1, the ratio of nearest to next-nearest-neighbor couplings is set by R_c (Fig. 1).

While the Rydberg dressing is subject to dissipation from the finite lifetime Γ^{-1} of the Rydberg state [43, 44], the interaction-to-decay ratio can be large [49, 50] in a 1D system. At fixed Rabi frequency Ω, the ratio of the Ising coupling J to the lifetime $\gamma = (\Omega^2/4\Delta^2)\Gamma$ of the Rydberg-dressed state is limited to $J/\gamma = \frac{\Omega^2}{2\Delta\Gamma} < \frac{\Omega}{\Gamma}$. This limit is set by the condition $\Omega^2/\Delta^2 \ll 1$ that the Rydberg-state population within the radius $R_c \sim a_1$ be small, so that the perturbative result of Eq. 4 holds. At realistic laser power on the $6S_{1/2} \to nP_{3/2}$ transitions (with $n \gtrsim 40$) in cesium [85], parameters $(\Omega, \Gamma) \approx 2\pi \times (4, 0.002)$ MHz allow for large coupling-to-decay ratios $J/\gamma \lesssim 10^3$.

To observe the FSPT phase, we envision initializing the system in a product state with high energy density and letting it undergo unitary time evolution. After each Floquet period T, one measures the spin-spin autocorrelation function $\langle\sigma^\alpha(nT)\sigma^\alpha(0)\rangle$ for both an edge and bulk spin. Numerics (Fig. 3c) for $N = 10$ atoms indicate that a time $t \sim 10^2/J$ suffices to observe a significant difference between the bulk- and edge-spin fidelities. The difference can be observed over an even shorter time scale $t \sim 30/J$ (Fig. 3d) by adding a decohering interaction term $V_x\sum_i \sigma_i^x\sigma_{i+1}^x$ to H_1 in Eqn. 3. Experimentally, V_x can be introduced by simultaneously dressing both states $|\downarrow\rangle$ and $|\uparrow\rangle$ [50] to generate flip-flop processes $\propto \sigma_i^+\sigma_{i+1}^-$.

To experimentally verify the distinct advantages of the intrinsically Floquet SPT phase, our scheme can be modified to emulate the ESPT for comparison. Realizing the ESPT Hamiltonian requires alternating stroboscopically between ferromagnetic and antiferromagnetic Ising interactions by simultaneously changing the signs of the detuning Δ and of the van der Waals coefficient C_6. While a conceptually simple approach is to switch between two different laser fields detuned by $\Delta_2 \approx -\Delta_1$ from two different Rydberg states $|\mathcal{R}_2\rangle, |\mathcal{R}_1\rangle$, a more practical approach may be to dynamically control the sign of C_6 with an electric field [86]. We detail concrete level schemes for an implementation in cesium in [71].

[1] B. A. Bernevig, T. L. Hughes, and S.-C. Zhang, Science **314**, 1757 (2006).
[2] Y. Chen, J. Analytis, J.-H. Chu, Z. Liu, S.-K. Mo, X.-L. Qi, H. Zhang, D. Lu, X. Dai, Z. Fang, *et al.*, Science **325**, 178 (2009).
[3] M. Z. Hasan and C. L. Kane, Reviews of Modern Physics **82**, 3045 (2010).
[4] X.-L. Qi and S.-C. Zhang, Reviews of Modern Physics **83**, 1057 (2011).
[5] B. Bernevig and T. Hughes, *Topological Insulators And Topological Superconductors* (Princeton University Press, 2013).
[6] C. L. Kane and E. J. Mele, Physical review letters **95**, 146802 (2005).
[7] J. E. Moore and L. Balents, Physical Review B **75**, 121306 (2007).
[8] T. Senthil, Annual Review of Condensed Matter Physics **6**, 299 (2015), http://dx.doi.org/10.1146/annurev-conmatphys-031214-014740.
[9] A. M. Turner and A. Vishwanath, arXiv:1301.0330 (2013).
[10] X. Chen, Z.-C. Gu, and X.-G. Wen, Physical Review B **83**, 035107 (2011).
[11] W. J. L. Buyers, R. M. Morra, R. L. Armstrong, M. J. Hogan, P. Gerlach, and K. Hirakawa, Phys. Rev. Lett. **56**, 371 (1986).
[12] R. M. Morra, W. J. L. Buyers, R. L. Armstrong, and K. Hirakawa, Phys. Rev. B **38**, 543 (1988).
[13] G. Xu, J. F. DiTusa, T. Ito, K. Oka, H. Takagi, C. Broholm, and G. Aeppli, Phys. Rev. B **54**, R6827 (1996).
[14] W. S. Bakr, J. I. Gillen, A. Peng, S. Fölling, and M. Greiner, Nature **462**, 74 (2009).
[15] M. Atala, M. Aidelsburger, J. T. Barreiro, D. Abanin, T. Kitagawa, E. Demler, and I. Bloch, Nature Physics **9**, 795 (2013).
[16] L. W. Cheuk, M. A. Nichols, M. Okan, T. Gersdorf, V. V. Ramasesh, W. S. Bakr, T. Lompe, and M. W. Zwierlein, Physical review letters **114**, 193001 (2015).
[17] E. Haller, J. Hudson, A. Kelly, D. A. Cotta, B. Peaudecerf, G. D. Bruce, and S. Kuhr, Nature Physics **11**, 738 (2015).
[18] M. F. Parsons, A. Mazurenko, C. S. Chiu, G. Ji, D. Greif, and M. Greiner, Science **353**, 1253 (2016).
[19] A. Chandran, V. Khemani, C. R. Laumann, and S. L. Sondhi, Phys. Rev. B **89**, 144201 (2014).
[20] Y. Bahri, R. Vosk, E. Altman, and A. Vishwanath, Nature Communications **6**, 7341 (2015).
[21] N. Y. Yao, C. R. Laumann, and A. Vishwanath, arXiv:1508.06995 [cond-mat, physics:quant-ph] (2015), arXiv: 1508.06995.
[22] T. Iadecola, L. H. Santos, and C. Chamon, Physical Review B **92**, 125107 (2015).
[23] V. Khemani, A. Lazarides, R. Moessner, and S. L. Sondhi, Phys. Rev. Lett. **116**, 250401 (2016).
[24] C. W. von Keyserlingk and S. L. Sondhi, Phys. Rev. B **93**, 245145 (2016).
[25] C. W. von Keyserlingk and S. L. Sondhi, Phys. Rev. B **93**, 245146 (2016).
[26] A. C. Potter, T. Morimoto, and A. Vishwanath, Phys. Rev. X **6**, 041001 (2016).
[27] D. V. Else and C. Nayak, Phys. Rev. B **93**, 201103 (2016).
[28] R. Roy and F. Harper, Phys. Rev. B **94**, 125105 (2016).
[29] M. Aidelsburger, M. Atala, S. Nascimbène, S. Trotzky, Y.-A. Chen, and I. Bloch, Phys. Rev. Lett. **107**, 255301 (2011).
[30] G. Jotzu, M. Messer, R. Desbuquois, M. Lebrat, T. Uehlinger, D. Greif, and T. Esslinger, Nature **515**, 237 (2014).
[31] C. J. Kennedy, W. C. Burton, W. C. Chung, and W. Ketterle, Nat Phys **11**, 859 (2015).
[32] T. Oka and H. Aoki, Phys. Rev. B **79**, 081406 (2009).
[33] N. H. Lindner, G. Refael, and V. Galitski, Nature Physics **7**, 490495 (2011).
[34] Y. H. Wang, H. Steinberg, P. Jarillo-Herrero, and N. Gedik, Science **342**, 453 (2013).
[35] M. C. Rechtsman, J. M. Zeuner, Y. Plotnik, Y. Lumer, D. Podolsky, F. Dreisow, S. Nolte, M. Segev, and A. Szameit, Nature **496**, 196 (2013).
[36] P. Titum, N. H. Lindner, M. C. Rechtsman, and G. Refael, Phys. Rev. Lett. **114**, 056801 (2015).
[37] N. R. Cooper, Phys. Rev. Lett. **106**, 175301 (2011).
[38] P. Hauke, O. Tieleman, A. Celi, C. Ölschläger, J. Simonet, J. Struck, M. Weinberg, P. Windpassinger, K. Sengstock, M. Lewenstein, and A. Eckardt, Phys. Rev. Lett. **109**, 145301 (2012).
[39] N. Fläschner, B. Rem, M. Tarnowski, D. Vogel, D.-S. Lühmann, K. Sengstock, and C. Weitenberg, Science **352**, 1091 (2016).
[40] L. W. Clark, L.-C. Ha, C.-Y. Xu, and C. Chin, Phys. Rev. Lett. **115**, 155301 (2015).
[41] C. Gaul, B. J. DeSalvo, J. A. Aman, F. B. Dunning, T. C. Killian, and T. Pohl, Phys. Rev. Lett. **116**, 243001 (2016).
[42] Y. Y. Jau, A. M. Hankin, T. Keating, I. H. Deutsch, and G. W. Biedermann, Nat Phys **12**, 71 (2016).
[43] J. Zeiher, R. van Bijnen, P. Schauß, S. Hild, J.-y. Choi, T. Pohl, I. Bloch, and C. Gross, Phys. Rev. X **5**, 031015 (2015).
[44] E. A. Goldschmidt, T. Boulier, R. C. Brown, S. B. Koller, J. T. Young, A. V. Gorshkov, S. L. Rolston, and J. V. Porto, Phys. Rev. Lett. **116**, 113001 (2016).
[45] H. Labuhn, D. Barredo, S. Ravets, S. de Léséleuc, T. Macrì, T. Lahaye, and A. Browaeys, Nature **534**, 667 (2016).
[46] J. Zeiher, J.-y. Choi, A. Rubio-Abadal, T. Pohl, R. van Bijnen, I. Bloch, and C. Gross, arXiv preprint arXiv:1705.08372 (2017).
[47] H. Bernien, S. Schwartz, A. Keesling, H. Levine, A. Omran, H. Pichler, S. Choi, A. S. Zibrov, M. Endres, M. Greiner, V. Vuleti, and M. D. Lukin, arXiv preprint arXiv:1707.04344 (2017).
[48] N. Y. Yao, A. V. Gorshkov, C. R. Laumann, A. M. Läuchli, J. Ye, and M. D. Lukin, Phys. Rev. Lett. **110**,

185302 (2013).
[49] R. van Bijnen and T. Pohl, Phys. Rev. Lett. **114**, 243002 (2015).
[50] A. W. Glaetzle, M. Dalmonte, R. Nath, C. Gross, I. Bloch, and P. Zoller, Phys. Rev. Lett. **114**, 173002 (2015).
[51] S. Fazzini, A. Montorsi, M. Roncaglia, and L. Barbiero, arXiv preprint arXiv:1607.05682 (2016).
[52] J. E. Johnson and S. L. Rolston, Phys. Rev. A **82**, 033412 (2010).
[53] N. Henkel, R. Nath, and T. Pohl, Phys. Rev. Lett. **104**, 195302 (2010).
[54] G. Pupillo, A. Micheli, M. Boninsegni, I. Lesanovsky, and P. Zoller, Phys. Rev. Lett. **104**, 223002 (2010).
[55] L. I. R. Gil, R. Mukherjee, E. M. Bridge, M. P. A. Jones, and T. Pohl, Phys. Rev. Lett. **112**, 103601 (2014).
[56] L. D'Alessio and M. Rigol, Phys. Rev. X **4**, 041048 (2014).
[57] A. Lazarides, A. Das, and R. Moessner, Physical Review E **90**, 012110 (2014).
[58] D. M. Stamper-Kurn, Physics **2**, 80 (2009).
[59] D. A. Huse, R. Nandkishore, V. Oganesyan, A. Pal, and S. L. Sondhi, Physical Review B **88**, 014206 (2013).
[60] R. Nandkishore and D. A. Huse, Annual Review of Condensed Matter Physics **6**, 15 (2015).
[61] E. Altman and R. Vosk, Annual Review of Condensed Matter Physics **6**, 383 (2015).
[62] P. Ponte, A. Chandran, Z. Papi, and D. A. Abanin, Annals of Physics **353**, 196 (2015).
[63] M. Barkeshli, N. Y. Yao, and C. R. Laumann, Phys. Rev. Lett. **115**, 026802 (2015).
[64] T. Kitagawa, E. Berg, M. Rudner, and E. Demler, Physical Review B **82**, 235114 (2010).
[65] L. Jiang, T. Kitagawa, J. Alicea, A. R. Akhmerov, D. Pekker, G. Refael, J. I. Cirac, E. Demler, M. D. Lukin, and P. Zoller, Physical Review Letters **106**, 220402 (2011).
[66] A. Russomanno and E. G. D. Torre, EPL (Europhysics Letters) **115**, 30006 (2016).
[67] M. S. Rudner, N. H. Lindner, E. Berg, and M. Levin, Physical Review X **3**, 031005 (2013).
[68] T. E. Lee, Y. N. Joglekar, and P. Richerme, Phys. Rev. A **94**, 023610 (2016).
[69] F. D. M. Haldane, Physical Review Letters **50**, 1153 (1983).
[70] Any driving function that changes sign every half-period will suffice. For instance, tweaking the binary drive from [23] to have this property would also yield an ESPT.
[71] See supplementary information for details.
[72] D. A. Abanin, W. De Roeck, and F. Huveneers, Phys. Rev. Lett. **115**, 256803 (2015).
[73] T. Kuwahara, T. Mori, and K. Saito, Annals of Physics **367**, 96 (2016).
[74] D. Abanin, W. De Roeck, F. Huveneers, and W. W. Ho, arXiv preprint arXiv:1509.05386 (2016).
[75] Note that for finite frequency drives, the n^{th} order perturbative correction to $H_{\text{F}}^{(0)}$ is of order $1/\omega^n$.
[76] A. Y. Kitaev, Physics-Uspekhi **44**, 131 (2001).
[77] The fields for the ESPT are sampled from uniform distributions with $\langle h_{\text{bulk}}\rangle = 1.0$ and width $\delta h_{\text{bulk}} = 2.0$ in the bulk ($1 < i < N$); $\langle h_{\text{edge}}\rangle = a(\lambda_1, \lambda_2)/J_0(2\lambda_1) \approx -0.11$ and width $\delta h_{\text{edge}} = 2\langle h_{\text{edge}}\rangle$ on the edges.
[78] For each disorder realization, we numerically obtain $F^{\alpha}(t)$, fit an exponential e^{-t/T_2^*} through the peaks, extract T_2^*, and average over 30-1000 realizations.
[79] V. M. Bastidas, C. Emary, G. Schaller, and T. Brandes, Phys. Rev. A **86**, 063627 (2012).
[80] M. Thakurathi, A. A. Patel, D. Sen, and A. Dutta, Phys. Rev. B **88**, 155133 (2013).
[81] For each disorder realization, we diagonalize the Floquet Hamiltonian H_{F} defined via $U = e^{-iH_{\text{F}}T}$ and obtain a set of quasi-energies ϵ_n modulo 2π. We define the energy gaps as $\delta_n = \epsilon_{n+1} - \epsilon_n$ and the ratio $r = \min(\delta_n, \delta_{n+1})/\max(\delta_n, \delta_{n+1})$. Finally, we average over all the quasi-energies and over 2500-100000 disorder realizations.
[82] N. Y. Yao, C. R. Laumann, S. Gopalakrishnan, M. Knap, M. Müller, E. A. Demler, and M. D. Lukin, Phys. Rev. Lett. **113**, 243002 (2014).
[83] B. J. Lester, N. Luick, A. M. Kaufman, C. M. Reynolds, and C. A. Regal, Physical review letters **115**, 073003 (2015).
[84] M. Endres, H. Bernien, A. Keesling, H. Levine, E. R. Anschuetz, A. Krajenbrink, C. Senko, V. Vuletic, M. Greiner, and M. D. Lukin, arXiv:1607.03044[quant-ph] (2016).
[85] J. Lee, M. J. Martin, Y.-Y. Jau, T. Keating, I. H. Deutsch, and G. W. Biedermann, arXiv preprint arXiv:1609.03940 (2016).
[86] T. Vogt, M. Viteau, J. Zhao, A. Chotia, D. Comparat, and P. Pillet, Phys. Rev. Lett. **97**, 083003 (2006).